Zirconium Trisulfide as a Promising Cathode Material for Li Primary Thermal Batteries

Kyriakos Giagloglou,[a] Julia L. Payne,[a] Christina Crouch,[b] Richard K. B. Gover,[b] Paul A. Connor,[a] and John T. S. Irvine[a,*,z]

[a]*University of St. Andrews, School of Chemistry, St Andrews Fife KY16 9ST, United Kingdom*
[b]*AWE, Aldermaston, Reading RG7 4PR, United Kingdom*

In this work ZrS_3 has been synthesized by solid state reaction in a sealed quartz tube and investigated as a candidate cathode material in Li thermal batteries. The structure of ZrS_3 before and after cell testing has been studied using powder X-ray diffraction. A new spinel related material, $LiZr_2S_4$, has been identified as the product of the electrochemical process, which can be indexed to a = 10.452(8) Å cubic unit cell. The electrochemical properties of the batteries were investigated at 500°C against $Li_{13}Si_4$ by galvanostatic discharge and galvanostatic intermittent titration technique (GITT). In a thermal Li cell at 500°C a single voltage plateau of 1.70 V at a current density of 11 mA/cm^2 was achieved with capacity of 357 mA h g^{-1}. Therefore ZrS_3 material has some promise as a cathode for Li thermal batteries.

Manuscript submitted October 3, 2016; revised manuscript received November 15, 2016. Published November 25, 2016.

Thermal batteries are electrochemical devices that convert chemical energy directly to electrical energy by an electrochemical oxidation-reduction reaction at high temperature utilizing a molten salt electrolyte. The electrolyte is only ionically conductive when is molten and the batteries remain active while the electrolyte stays molten. Like all primary batteries they consist of an anode, an electrolyte-separator and a cathode. The advantage of using thermal batteries is that the electrolyte is solid and poor ionic and electronic conductors at room temperature, which as a result provides stable energy storage for decades.[1] The elevated temperature also enhances the electrochemical kinetics to provide higher power as they can be discharged at higher currents. The most common applications of thermal batteries are those that need a long shelf life but need instantly high power like emergency power systems, such as in pilot ejector seats and sonobuoys.

Until now thermal batteries use a high melting point lithium alloy ($Li_{13}Si_4$) as the anode, a halide salt eutectic bound in an insulating porous material as the electrolyte, and a 1st row transition metal sulfide as the cathode. In this work the $Li_{13}Si_4$ alloy is used as an anode as it has the highest Li content and is the least moisture sensitive of the lithium silicon alloys. The anode $Li_{13}Si_4$ or ($x = 3.25$ in the formula of Li_xSi) is stable and exhibits a potential of 0.157 V against Li metal at 415°C. During discharge process a phase transition takes place $Li_{13}Si_4$ to Li_7Si_3 corresponds to 3.66 Li^+ / mole of Li – Si and the capacity of this alloy is 485 mA h g^{-1}.[2] The most common electrolyte for use in thermal batteries is the lithium chloride – potassium chloride eutectic (LiCl 44.8 wt%–55.2 wt% KCl) with a melting point of ~354°C and this requires a minimum of 35 wt% MgO as separator.[3] MS_2 sulfides where M is Fe, Ni or Co are the most studied cathodes and they have potentials vs $Li_{13}Si_4$ at around 1.70 V for their first electrochemical transition but also have further electrochemical transitions, which eventually ends in complete reduction to the metal.[4]

This work investigates ZrS_3 as a possible cathode material for use in Li thermal batteries. The synthesis of ZrS_3 has previously been reported by many authors[5–8] and the synthetic procedure (*via* a conventional solid state route) involved multiple firings at temperatures from 600°C–1000°C for 1 to 25 days. The work recently had success in synthesizing the sample in shorter time using one firing step.

This material has a pseudo one-dimensional structure (Figure 1) and Zr atoms occupy the center of a trigonal prism with sulfur atoms at the corners and two of those S atoms bond to each other. Neighboring atoms create an infinite chain along the *b*-axis of the crystal. The large inter-chain distances results in weak inter-chain interactions. This leads to this family of materials possessing anisotropic material properties.[9] These chains stack to form corrugated layers perpendicular to *c*-axis. The aim of this work is to synthesize and characterize ZrS_3 and to fabricate into cells in order to test at high temperature vs $Li_{13}Si_4$ using a variety of discharge conditions.

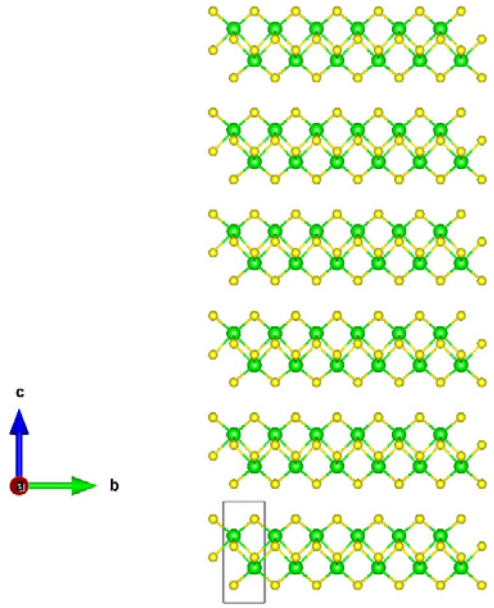

Figure 1. Crystal structure of ZrS_3. Yellow atoms are sulfur, green atoms are zirconium.

Experimental

ZrS_3 was synthesized by a solid state reaction in sealed quartz tube to prevent oxidation of the starting materials. 0.966 g of zirconium (Aldrich,-100 mesh) and 1.026 g of sulfur (Alfa Aesar,-100 mesh, 99.5%) powders were used. All the powders were weighed out and mixed in a mortar and pestle in air and then sealed into an evacuated (10^{-3} mbar) quartz tube before the reactions were carried out inside a tube furnace. The compound was fired at 730°C for 1 week, with a heating and cooling rate of 1°C min^{-1} used.

Room temperature powder X-ray diffraction data was collected using a Panalytical Empyrean diffractometer in Bragg-Bretano geometry with a Ge (220) monochromator and Cu Kα_1 radiation (λ = 1.5406 Å). Data was collected from 5° to 70° 2θ for 1 hour with a

*Electrochemical Society Member.
[z]E-mail: jtsi@st-and.ac.uk

step size of 0.017° and a time per step of 0.94 seconds. Variable temperature powder X-ray diffraction data was collected using a Panalytical Empyrean diffractometer with Mo $K\alpha_{1,2}$ radiation, ß-filter and an X'celerator RTMS detector, equipped with an Anton Paar HTK1200N furnace. Data was collected from 4° to 40° 2θ for 6 hours with a step size of 0.008° and a time per step of 600 seconds. The ZrS_3 sample was loaded into a quartz capillary and sealed for variable temperature data collection. WinXPOW software was used for indexing and refining the unit cell parameters. Scanning electron microscopy was carried out using a JEOL JSM-5600 microscope to study the morphology and composition of the cathode powder.

Fabrication of the composite cathode for high temperature electrochemical investigation was made by mixing 75 wt% (0.15 g) ZrS_3 and 25 wt% (0.05 g) Super P Carbon. 45 wt% MgO and 55 wt% LiCl-KCl eutectic (Sigma Aldrich, 99.99%, LiCl 44.8 wt% – 55.2 wt% KCl) were ball milled under argon make the separator/electrolyte (0.2 g). The anode was made by mixing 75 wt% (0.15 g) $Li_{13}Si_4$ (Lithium Rockwood) and 25 wt% (0.05 g) LiCl-KCl eutectic. This amount is in excess to keep the discharge on the first anode plateau for the amount of cathode used. The cathode, anode and electrolyte/separator mixtures were individually pressed into pellets of diameter 13 mm at 5 tonnes for 3 minutes. The anode, separator/electrolyte and cathode pellets were held in place using an alumina cup and graphite foil was used as current collectors. The cell assembly was placed in a Swagelok fitting, to allow measurements to be carried out under an inert atmosphere. Cell testing was carried out at 500°C which is above the melting point of the LiCl-KCl molten salt electrolyte. The electrochemical cells were tested at elevated temperature and were investigated electrochemically by a Maccor battery tester Model 5300 by galvanostatic discharge. Thermal cells were also tested by the galvanostatic intermittent titration technique (GITT). In order to have sufficiently slow potential changes a current density of 7.5 mA/cm^2 was chosen for discharge for the GITT measurements. The experimental capacity was calculated using the Maccor software and then this was converted to x, the moles of lithium ions per moles of formula unit.

Results and Discussion

Cathode material characterization.—Zirconium trisulfide was studied by a powder X-Ray diffraction in both reflection and transmission geometry with the data shown in Figures 2a and 2b. The sample was confirmed to be a single phase and could be indexed to the $P2_1/m$ unit cell reported by Furuseth et al. Cell parameters were refined using the WinXPOW software and are given in Table I. In order to investigate the stability of ZrS_3 at elevated temperature, XRD data were collected in situ at temperatures in the range from 25°C to 500°C as shown in Figure 3a. Throughout this temperature range ZrS_3 is stable and there are no phase transformations or apparent degradation. The volume of the unit cell increases as the temperature increases as shown in Figure 3b.

The morphology of ZrS_3 was investigated by SEM and is presented in Figures 4a and 4b. Figure 4b is at higher magnification than Figure 4a and shows that the crystallites have a uniform morphology, which is consistent with a single phase sample and the crystallites are needles. The shape of the ZrS_3 grains gives a high surface are which could enable lithium ion diffusion in the thermal cell at high temperatures.

Table I. Refined unit cell parameters of ZrS_3.

Unit cell [Å]	Experimental	Published[5]
a	5.125(5)	5.124
b	3.625(4)	3.624
c	8.981(10)	8.980
β [°]	97.29(8)	97.28
Cell Volume [Å^3]	165.53(21)	165.44

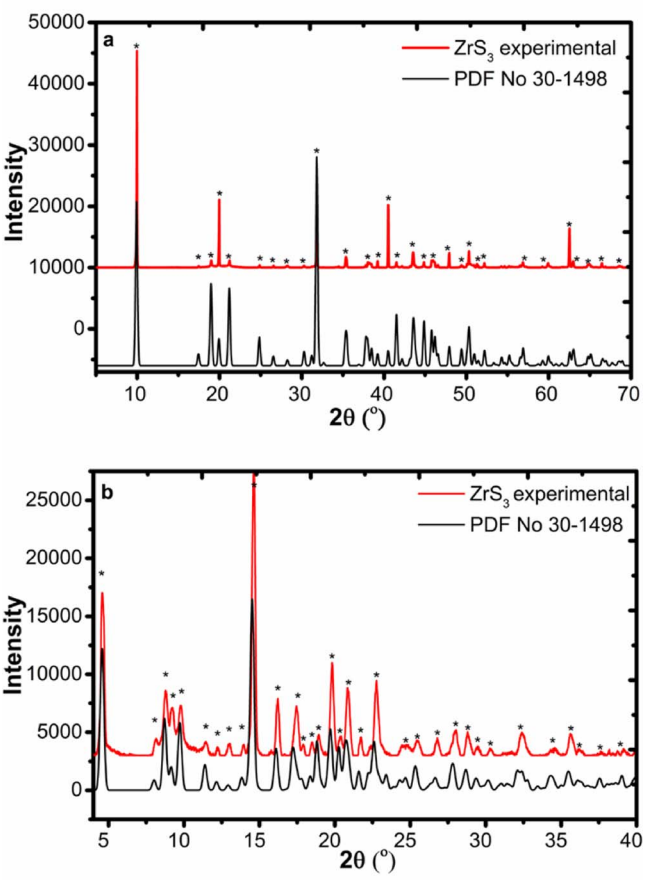

Figure 2. XRD data (Cu radiation) of ZrS_3 (reflection) (red line) (a) and XRD data (Mo radiation) of ZrS_3 (transmission geometry in a capillary) (red line) (b) compared to the simulated diffraction pattern of ZrS_3 using the published crystallographic model[5] (black line). The experimental intensity is different from the intensities in the simulated diffraction due to the needle like ZrS_3 morphology which results in a large effect due to preferred orientation.

EDX analysis confirms the average elemental composition of ZrS_3 with zirconium 25 at% and sulfur 75 at%.

The needle-like shape of the ZrS_3 crystals results in a large effect on the diffraction pattern from preferred orientation, and as a result, collecting data in a capillary rather than a pressing into a bulk flat plate sample holder, allowed the collection of data with a much better sampling of intensities. To test the temperature stability of zirconium trisulfide even further, a quantity of ZrS_3 was heated to 700°C at 6°C min^{-1} and was held at this temperature for 1 hour under flowing argon. Then it was cooled to room temperature at 6°C min^{-1}. The resulting diffraction pattern is shown in Figure 5. The diffraction data shows that ZrS_3 had decomposed to ZrS_2. ZrS_2 crystallizes in space group $P\bar{3}m1$ and the refined cell parameters were $a = b = 3.6631(4)$ Å, $c = 5.8331(5)$ Å. This is in agreement with Fotouhi.[10] The mass of ZrS_3 before heating was 0.1597 g and it lost a mass of 0.0435 g after heating to 700°C. This mass loss of 27% is consistent with the thermal decomposition of ZrS_3 to ZrS_2 and gaseous sulfur at elevated temperatures.

Electrochemical investigation of ZrS_3 at 500°C.—ZrS_3 was characterized electrochemically by galvanostatic discharge and galvanostatic intermittent titration technique. Galvanostatic discharge curves of the ZrS_3 cathode material at 500°C are presented in Figure 6a. ZrS_3 was discharged at different current densities (7.5, 11, 15, 19, 23 and 75 mA/cm^2) to investigate the performance and the resulting discharge profiles. At both current densities of 7.5 and 11 mA/cm^2 there was a single flat voltage plateau at around 1.70 V and a capacity

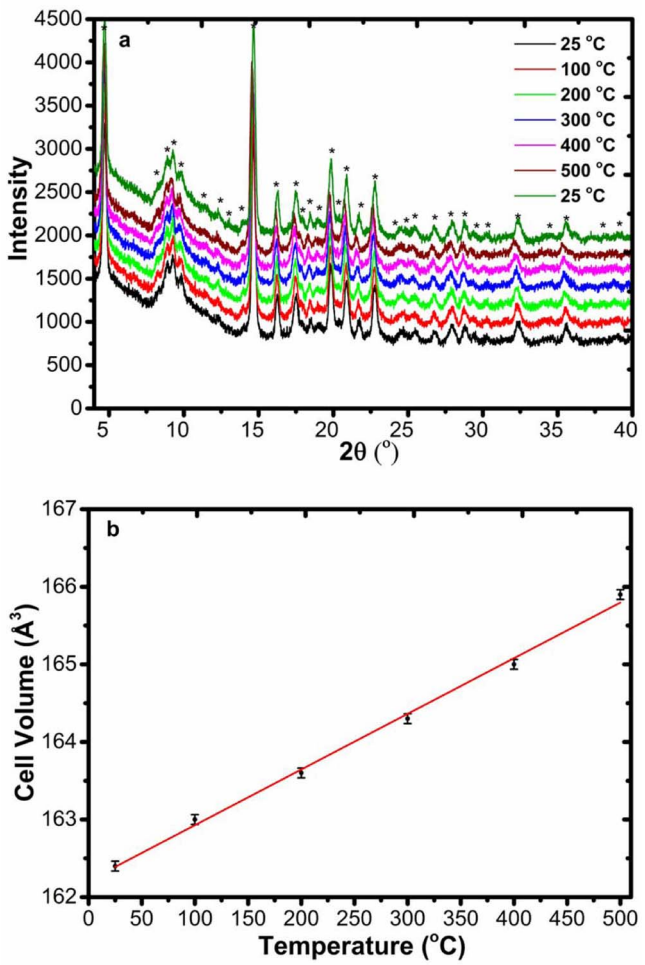

Figure 3. Variable temperature XRD data (Mo radiation) of ZrS_3 at temperatures from 25°C up to 500°C (a) and cell volume of ZrS_3 vs temperature from 25°C up to 500°C (b).

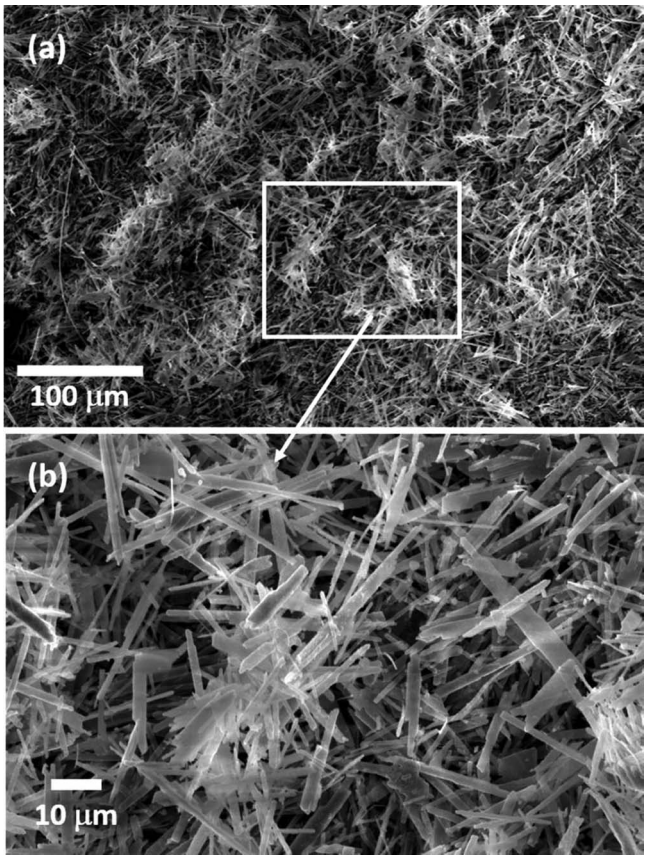

Figure 4. SEM images of ZrS_3.

of 357 mA h g^{-1} was achieved. 25 wt% Super P Carbon was added to the cathode to increase the electronic conductivity and the value of x number was 2.5. At current densities of 15, 19 and 23 mA/cm^2 it can be observed that the single flat voltage plateau is lower than 1.70 V as the cell resistance might be higher however the capacity is still high (over 300 mA h g^{-1}) and the value of x number was around 2.25. At a current density of 75 mA/cm^2 the single plateau is around 1.25 V and a capacity of around 200 mA h g^{-1} was achieved.

The amount of active anode (0.15 g) corresponds to 73 mA h for the discharge plateau from $Li_{13}Si_4$ to Li_7Si_3 which is 0.157 V vs Li. The measured capacity of the cathode is 54 mA h which keeps the discharge as being performed against the 0.157 V Li plateau.

According to the electrochemical reaction the result is $2ZrS_3 + 5Li \Rightarrow 2Li_2S + LiZr_2S_4$.

GITT testing consists of galvanostatic discharge pulses, each 10 minutes long, followed by 5 minutes of relaxation time, with no current passing through the cell[11,12] as shown in Figure 6b. The potential drops between the pulses and the relaxation until a potential of 1 V is reached. The IR drop is 0.05 V at the beginning of discharge and 0.125 V at the end of the measurement, which indicates that the cell resistance is increasing during the reduction of the cathode, from a resistance of around 6 Ω at the beginning of the measurement to around 16 Ω after the cell discharge, which suggests that it is more difficult to insert lithium ions to the structure of the cathode electrode.

Compared to MS_2 cathodes such as FeS_2, NiS_2 or CoS_2, the ZrS_3 has a good voltage profile, a good capacity of 357 mA h g^{-1}, a good thermal stability and most importantly a single flat voltage plateau at 1.70 V vs $Li_{13}Si_4$ at 500°C as shown in Table II. Moreover CoS_2 decomposes to Co_3S_4 at 650°C,[13] NiS_2 decomposes to NiS at 600°C[14] and FeS_2 decomposes to FeS at 580°C. Sulfur gas in all cases is released and reacts exothermally with the anode electrode or dissolved lithium in the chosen molten salt electrolyte.[15,16] In the discharge reactions of NiS_2 and CoS_2 against $Li_{13}Si_4$ no lithiated products are formed. In the case of FeS_2 and ZrS_3 lithiated products such as $Li_3Fe_2S_4$, Li_2FeS_2 and $LiZr_2S_4$, respectively are formed. CoS_2 exhibits capacity of 598 mA h g^{-1}, FeS_2 exhibits capacity of 558 mA h g^{-1} and NiS_2 exhibits capacity of 545 mA h g^{-1}[14] as shown in Table II.

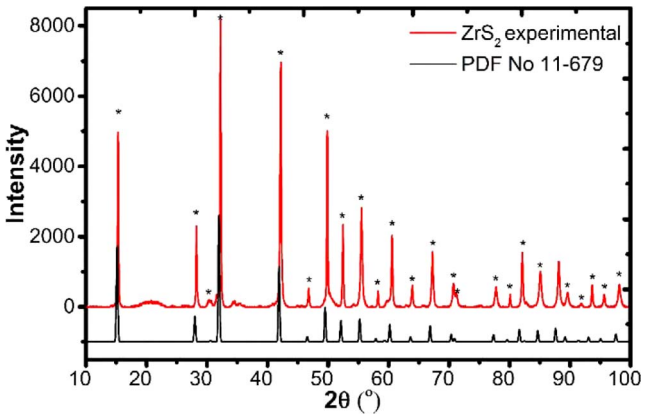

Figure 5. XRD data (Cu radiation) of thermal decomposition of ZrS_3 to ZrS_2 (red line) compared to the simulated diffraction pattern of ZrS_2 using the published crystallographic model[10] (black line).

Table II. Capacity, voltages and thermal decomposition of ZrS_3 compared to FeS_2, CoS_2 or NiS_2.

Sulfides	Capacity (mA h g^{-1})	Thermal decomposition	Voltages against Li – Si at 500°C
FeS_2	558[4]	$FeS_2 \Rightarrow FeS + \frac{1}{2} S_2$ at 580°C[15,16]	1.77 V, 1.64 V, 1.13 V[17]
CoS_2	598[4]	$3\,CoS_2 \Rightarrow Co_3S_4 + S_2$ at 650°C[13]	1.75 V, 1.40 V, 1.25 V[17]
NiS_2	545[4]	$NiS_2 \Rightarrow NiS + \frac{1}{2} S_2$ at 600°C[14]	1.76 V, 1.60 V, 1.40 V, 1.25 V[17]
ZrS_3	357	$ZrS_3 \Rightarrow ZrS_2 + \frac{1}{2} S_2$ at 700°C	1.70 V

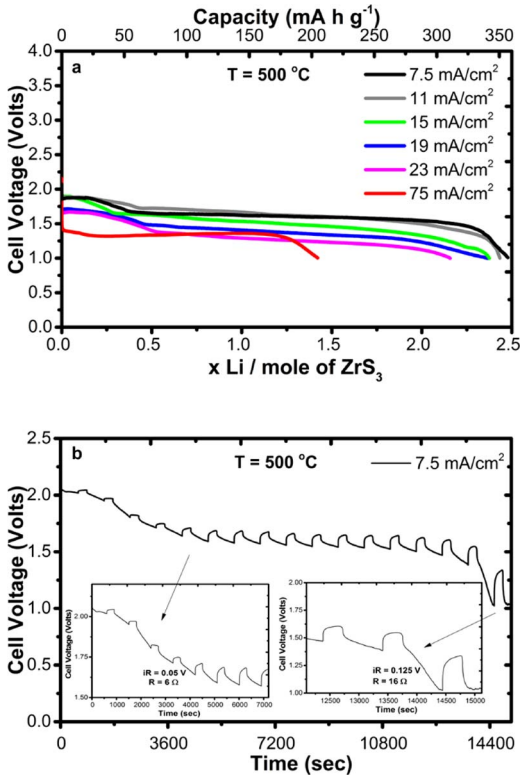

Figure 6. Galvanostatic discharge of ZrS_3 at current densities of 7.5, 11, 15, 19, 23 and 75 mA/cm^2 at 500°C (a) and galvanostatic intermittent titration technique of ZrS_3 at current density of 7.5 mA/cm^2 at 500°C (b).

XRD data were collected on the cathode after discharge. The diffraction pattern shows peaks from a number of different phases due to the difficulty in separating the cathode from the electrolyte/separator after battery testing. A number of peaks were present in the diffraction pattern after battery testing, which could not be assigned to any known crystalline phase in the PDF database. These peaks could be indexed to a cubic unit cell, with cell parameters $a = 10.452(8)$ Å and space group $Fd\bar{3}m$ and suggests a spinel structure. Therefore, a new phase with a cubic structure forms during discharge as shown in Figure 7. The SEM image of the cathode after discharge shows that the crystallites are not needles, indicating a morphology very different to that observed before testing. EDX analysis on individual grains can confirm a new phase with a composition of zirconium 34 at% and sulfur 66 at% as shown in Figure 8.

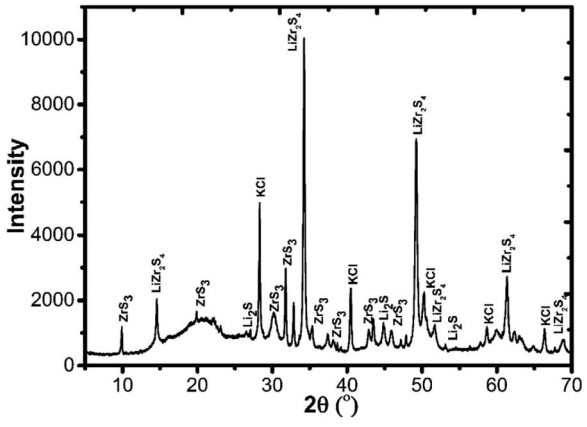

Figure 7. XRD data of the cathode electrode after discharge. There are some peaks from the starting material ZrS_3, some peaks of the electrolyte KCl and some sharp peaks of the new cubic phase $LiZr_2S_4$.

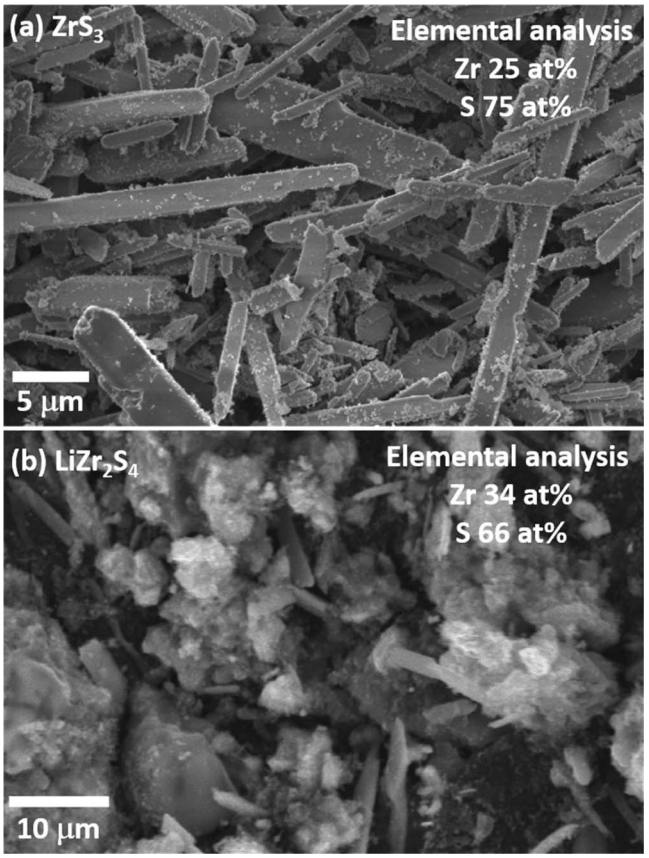

Figure 8. SEM image of cathode electrode before (a) and after (b) discharge.

Conclusions

Zirconium trisulfide has been synthesized by solid state reaction and tested as a cathode in Li thermal batteries. The high temperature discharge behavior is presented in this work. At 500°C the value of the working voltage plateau was measured for different current densities of 7.5, 11, 15, 19, 23 and 75 mA/cm^2. The GITT method showed that the cell resistance increased during the discharge. A new cubic phase $LiZr_2S_4$ was found after discharge with cell parameter $a = 10.452(8)$ Å. In the past a low temperature $Li_{0.5}ZrS_2$ phase was formed by Li insertion to ZrS_2 with a different polymorph structure.[18] The value of the single voltage plateau at 1.70 V when a current density of

both 7.5 and 11 mA/cm^2 was used can define ZrS_3 as promising candidate material for thermal batteries applications. Clearly a full understanding of the chemical composition and crystalline phases present post electrochemical testing is extremely important as it can lead to the discovery of new crystalline phases, whilst also providing insight into the electrochemical processes occurring during discharge.

Acknowledgments

Special thanks to AWE for their support and funding for this work. The authors acknowledge EPSRC Platform grant EP/K015540/1 and the Royal Society for a Wolfson Merit Award.

References

1. R. A. Guidotti and P. Masset, *J. Power Sources*, **161**, 1443 (2006).
2. C. J. Wen and R. A Huggins, *J. Solid State Chem.*, **37**, 271 (1981).
3. J. Sangster and A. D. Pelton, *J. Phys. Chem. Ref. Data*, **16**(3), 509 (1987).
4. S. K. Preto, Z. Tomczuk, S. von Winbush, and M. F. Roche, *J. Electrochem. Soc.*, **130**, 264 (1983).
5. S. Furuseth, L. Brattas, and A. Kjekshus, *Acta Chemica Scandinavica Series A*: **28**, 623 (1974); **29** (1975).
6. S. G. Patel, S. H. Chaki, and A. Agarwal, *Phys. Stat. Sol.*,**140**(a), 207 (1993).
7. W. Schairer and M. W. Shafer, *Phys. Status Solidi.*, **A17**, 181 (1973).
8. F. Levy and H. Berger, *J. Crystal Growth*, **61**, 61 (1983).
9. S. Srivastava and B. Avasthi. *J Mater Sci*., **27**, 3693 (1992).
10. Sieber K. Fotouhi, *Materials Research Bulletin*, **18**, 1477 (1983).
11. C. J. Wen, B. A. Boukamp, and R. A. Huggins, *J. Electrochem. Soc.*, **126**(12), 2258 (1979).
12. W. Weppner and R. A. Huggins, *J. Electrochem. Soc.*, **124**(10), 1569 (1977).
13. H. Rau, *J. Phys. Chem. Solids*, **37**, 931 (1976).
14. R. A. Guidotti, P. J. Nigrey, F. W. Reinhardt, and J. G. Odinek, *Proceedings of the 40th Power Sources Conference*, **250**, (2002).
15. M. C. Hash, J. A. Smaga, R. A. Guidotti, and F. W. Reinhardt, *Proceedings of the 8th International Symposium on Molten Salts*, **228**, (1992).
16. I. C. Hoare, H. J. Hurst, W. I. Stuart, and T. J. White, *J. Chem. Soc. Faraday Trans.*, **184**(9), 3071 (1988).
17. Patrick J. Masset and Ronald A. Guidotti, *Journal of Power Sources* **178**, 456 (2008).
18. W. R. McKinnon J. R. Dahn C Levy-Clement, *Solid State Communications*, **50**(2), 101 (1984).